Hot electron thermoreflectance coefficient of gold during electron-phonon nonequilibrium

Elizabeth L. Radue,[†,‡] John A. Tomko,[¶,‡] Ashutosh Giri,[†] Jeffrey L. Braun,[†] Xin Zhou,[§,‖] Oleg V. Prezhdo,[‖,⊥] Evan L. Runnerstrom,[#] Jon-Paul Maria,[#] and Patrick E. Hopkins[*,†,¶,@]

†*Department of Mechanical and Aerospace Engineering, University of Virginia, Charlottesville, VA, USA 22904*

‡*These authors contributed equally to this work*

¶*Department of Materials Science and Engineering, University of Virginia, Charlottesville, VA, USA 22904*

§*College of Environmental and Chemical Engineering, Dalian University, Dalian, P. R. China 116622*

‖*Department of Chemistry, University of Southern California, Los Angeles, CA, USA 90089*

⊥*Department of Physics and Astronomy, University of Southern California, Los Angeles, CA, USA 90089*

#*Department of Materials Science and Engineering, North Carolina State University, Raleigh, North Carolina 27695, USA*

@*Department of Physics, University of Virginia, Charlottesville, VA, USA 22904*

E-mail: phopkins@virginia.edu

Abstract

The temperature-dependent reflectivity of metals is quantified by the thermoreflectance coefficient, which is a material dependent parameter that depends on the metallic band struc-

ture, electron scattering dynamics, and photon wavelength. After short-pulse laser heating, the electronic sub-system in a metal can be driven to temperatures much higher than that of the lattice, which gives rise to unique non-equilibrium electron and phonon scattering dynamics, leading to a "hot electron" thermoreflectance that is different from the traditionally measured equilibrium coefficient. In this work, we analytically quantify and experimentally measure this hot electron thermoreflectance coefficient through ultrafast pump-probe measurements of thin gold films on silica glass and sapphire substrates. We demonstrate the ability to not only quantify the thermoreflectance during electron-phonon nonequilibrium, but also validate this coefficient's predicted dependence on the absolute temperature of the electronic subsystem. The approach outlined in this work provides a metrology to further understand and quantify excited-state scattering effects on the dielectric function of metals.

Keywords

Thermoreflectance, electron-phonon scattering, Pump-probe, electronic temperature, Drude model

Introduction

Thermoreflectance spectroscopy is a robust technique that has been used to interrogate the band structure and optical transitions in metals for decades.[1–8] In thermoreflectance spectroscopy, an oscillating temperature perturbation is applied to the sample of interest and the AC component of the reflected light is monitored. For example, in a standard optical pump-probe experiment, the pump is a modulated laser beam or train of laser pulses that is used to optically and thermally excite some sample at frequency, f, while the probe is used to interrogate the small changes in reflectivity of the sample caused by the pump excitation at frequency f. Due to the large electronic number density around the Fermi level in metals, this resulting thermoreflectivity change is related to characteristics of the electron population that is thermalizing, or thermalized, to a new distribution due to the pump excitation.

Hence, the thermoreflectance of the metal, defined as the change in reflectance due to a change in temperature, is given by

$$\frac{\Delta R}{R} = \frac{\Delta R}{R\left(T_0\right)} = \frac{R_{\text{excited}} - R\left(T_0\right)}{R\left(T_0\right)}, \tag{1}$$

where R is the reflectivity, T_0 is the baseline temperature of the sample, and R_{excited} is the reflectivity of the metal in the state during and after pump pulse absorption. The thermoreflectance of a metal is dictated by its thermoreflectance coefficient, dR/dT, which is typically small, on the order of $10^{-6} - 10^{-4}$ K^{-1} at room temperature and ambient conditions, its magnitude depending on the metallic band structure and the probe wavelength.[9–11] Therefore lock-in techniques are typically used to measure the thermoreflectance of metals in pump-probe geometries. Using ultrashort laser pulses in pump-probe geometries, the time evolution of the thermoreflectance can be measured.[12,13]

In Eq. 1, the parameter containing all of the pertinent electronic and atomistic information is R_{excited}, which is the reflectivity of the probe pulse after interacting with the metal in the excited state from the pump pulse. Upon pump pulse absorption, the electrons in the metal redistribute themselves to different electronic states depending on the energy of the photons absorbed by the metal; therefore, $R_{\text{excited}} = R\left(T_e, T_p\right)$ during pump absorption is related to the electronic band structure and available states for electron redistribution.[7,14–17] Upon and during thermalization (or partial thermalization)[18,19] the electron system can be described by an evolving electron temperature, T_e, which is greater than T_0 and different from the phonon temperature, T_p; this excited electron temperature and its evolution and decay is governed by the power of the pump pulse along with the electron dynamics and scattering mechanisms in the metal.[14,20–33]

Thus, monitoring the time evolution of the magnitude of the probe thermoreflectance signal gives an indirect indication of the electronic states and scattering dynamics in metals. This relationship underlies the principle of thermoreflectance-based measurement techniques, as the changes in electronic energies are related to the temperature evolution of the system. While the thermore-

flectance responses of various materials have been studied for quite some time,[34–36] direct experimental measurements of the thermoreflectance coefficients of materials using the short-pulsed measurement platforms employed in ultrafast and nanoscale energy transport measurements (e.g., time domain thermoreflectance (TDTR) and frequency domain thermoreflectance (FDTR))[37–41] have only become absolutely quantifiable recently.[9,10,42–44] However, these values for dR/dT using TDTR are measured during a temporal regime when the electrons and phonons have equilibrated and can be described with very similar temperatures (i.e., $T_e \approx T_p$). In other words, dR/dT is measured at pump-probe time delays hundreds of picoseconds after pulse absorption, orders of magnitude longer than the actual absorption event. For example, in a metal film, electron-phonon equilibrium occurs in the first several picoseconds after sub-picosecond pulse absorption, and dR/dT is typically measured at time delays on the order of hundreds of picoseconds. Since the reflectivity of materials depends on both the electronic and lattice temperatures $(R\left(T_e, T_p\right))$, the quantification of dR/dT_e independently of dR/dT_p would provide a unique avenue to study the electronic response of materials after short pulsed laser heating and during conditions of electron nonequilibria.

In this work, we quantify the "hot electron" thermoreflectance coefficient in gold films via monitoring the thermoreflectance of the gold during pump-probe TDTR measurements immediately after pulsed laser absorption. During this regime, the electrons in the Au are out of equilibrium with the gold lattice, and thus the condition $T_e \approx T_p$, usually assumed while reporting dR/dT values, is invalid. In this pump-probe time delay measurement regime, which is on the order of the sub-picosecond pulse duration, T_e can be much greater than T_p, allowing us to measure this hot electron thermoreflectance coefficient, dR/dT_e.

Using this approach applied to thin gold films on silica glass and sapphire substrates as experimental examples, we validate the linear electron temperature dependence of the thermoreflectance coefficient. Furthermore, we demonstrate a lattice temperature dependence in dR/dT_e. Traditionally, the non-linear reflectivity change in free electron metals has only been associated with changes in the electronic temperatures, and our lattice temperature dependence of the measured

dR/dT_e suggests this is not a complete picture. Indeed, as we derive below, an apparent non-linear temperature dependence could arise from a consequence of additional heating from the absorbed laser inducing a steady state temperature rise in thermally insulating substrates. This increase in lattice temperature in our TDTR experiments, driven by pulse accumulation,[45,46] has been a well established artifact of TDTR experiments on low thermal conductivity substrates, and our previous work has studied this effect on electron-phonon relaxation after short pulsed laser heating.[47] Our approach outlined in this work to directly quantify dR/dT_e allows us to study this effect on the ultrafast optical response directly, along with providing a metrology to further understanding the excited state scattering effects on the dielectric function of materials.

Theory of temperature dependence of dR/dT_e

Quantitatively, any thermoreflectance signal can be mathematically represented by a change in the baseline reflectivity of a sample surface resulting from a change in temperature of the sample (Eq. 1). The reflectivity of a material at the air (vacuum)/film interface is given by

$$R = \frac{(n_1 - 1)^2 + n_2^2}{(n_1 + 1)^2 + n_2^2} = \left| \frac{1 - \sqrt{\tilde{\epsilon}}}{1 + \sqrt{\tilde{\epsilon}}} \right|^2 \tag{2}$$

where n_1 and n_2 are the real (refractive index) and imaginary (extinction coefficient) parts of the complex index of refraction, $\tilde{n}$, and $\tilde{\epsilon}$ is the complex dielectric function. For an optical excitation that only promotes intraband transitions, such as free electron metals in the near infrared regime, we assume a Drude model for $\tilde{\epsilon}$, given by

$$\tilde{\epsilon}_f = 1 - \frac{\omega_{\text{plasma}}^2}{\omega\left(\omega + \frac{i}{\tau}\right)} \tag{3}$$

where ω is the frequency of light (i.e., 800 nm for this work), ω_{plasma} is the plasma frequency, and τ is the scattering time of the carriers interacting with the incoming light at frequency ω. Note, for the experimental measurements in this work on gold in which the thermoreflectivity is monitored

with a 800 nm pulse, the use of a Drude model to approximate $\tilde{\epsilon}$ is well established.[11,22,48–50]

The temperature dependence of the dielectric function, and thus temperature dependence of optical reflectivity, for metals is rooted in the temperature dependence of the electronic scattering rate, τ^{-1}. This relaxation time is dependent on both electron-electron (e-e) and electron-phonon (e-p) scattering rates and can be expressed as $\tau^{-1} = {\tau_{e-e}}^{-1} + {\tau_{e-p}}^{-1}$. For the free electron metal focus in this work, we make the common assumption that $\tau_{ee}^{-1} = A_{ee}T_e^2$ and $\tau_{ep}^{-1} = B_{ep}T_p$, where A_{ee} and B_{ep} are constants relating to electron-electron and electron-phonon scattering processes.[51] Note, the plasma frequency, ω_p, can also vary with respect to temperature and affect the dielectric function/optical reflectivity; as discussed in-depth in the Supporting Information, this weak temperature dependence does not contribute significantly for the laser parameters used in this work and can thus be considered constant with respect to temperature in our following derivations. Thus, taking the derivative of Eq. 2 with respect to T_e yields dR/dT_e. While this derivative is trivial in practice, especially with the use of any commercially available computing software (e.g., Mathematica), the analytical result is quite tedious. Thus, it is more intuitive to consider the series expansion of this result. Additionally, expansion about the absolute temperature may be more representative of values measured in such cases of non-equilibria; as stated via Eq. 1, pump-probe experiments measure the *change* in reflectivity due to pump excitation, not necessarily the differential, and are thus sensitive to absolute temperature at a given time delay rather than the fractional change in temperature. Expanding dR/dT_e about T_e and T_p yields

$$\frac{dR}{dT_e} \approx \sqrt{R}\left(\tilde{C} + \tilde{D}T_p\right)T_e \tag{4}$$

where $\tilde{C}$ and $\tilde{D}$ are both complex numbers that are functions of ω, ω_{plasma}, A_{ee}, and B_{ep} (note, $\tilde{C}$ and $\tilde{D}$ are presented in the Supporting Information). From Eq. 4, we see a trend that is in contrast with the typical assumption that the origin of a nonlinear reflectivity is only proportional to T_e^2. More specifically, when T_p is non-negligible relative to T_e, nonlinear dependence in the change in

reflectivity would be influenced by T_p, and thermoreflectance coefficient takes the form

$$\frac{dR}{dT_e} \approx \tilde{E}T_e + \tilde{F}T_pT_e. \tag{5}$$

However, from Eq. 5, when $T_p \ll T_e$,

$$\frac{dR}{dT_e} \approx \tilde{G}T_e \tag{6}$$

where $\tilde{E}$, $\tilde{F}$ and $\tilde{G}$ are functions of ω, ω_p, A_{ee}, B_{ep} and $\sqrt{R}$. Equation 6 implies that when $T_p \ll T_e$, the hot electron thermoreflectance coefficient should appear linear and lattice temperature independent, and thus, $\Delta R \propto T_e^2$. However, when T_p is large, additional non-linearities in ΔR could arise from lattice heating. Indeed, several previous reports of this nonlinear change in reflectivity were observed in thin Au films on amorphous SiO_2 substrates,[11,49,52] where the average absorbed power from the high repetition rate laser sources can lead to pulse-to-pulse accumulation of absorbed energy resulting in an appreciable steady state temperature rise, leading to phonon temperature rises well above ambient conditions.[47] Without explicit measurements of dR/dT_e, which we demonstrate in this work, the true behavior of ΔR with T_e would be left unverified experimentally. Our measurements of dR/dT_e, as described below, allow us to rectify this discrepancy in the nonequilibrium free electron response of materials.

Experimental measurement of dR/dT_e

The gold films studied in this work were 16 nm thick as confirmed with picosecond acoustics; the details of this analysis can be found in the Supporting Information.[53] The films were electron-beam evaporated on the amorphous SiO_2 and (0001) oriented single-crystal sapphire substrates after a light alcohol rinse and O_2 plasma clean to each substrate. The hot electron thermoreflectance coefficient was measured using a standard pump-probe TDTR configuration centered around a Ti:Sapphire oscillator with a 80 MHz repetition rate, center wavelength of 800 nm, and bandwidth of 10.5 nm.[37–41] The pump path is focused into a SHG BiB_3O_6 crystal,[54] converting the pump to

a 400 nm central wavelength. The probe path is directed down a mechanical delay stage, and the path length is varied to alter the temporal delay between the arrival of the probe beam relative to the pump beam on the sample surface. Thus, our measurements of dR/dT_e (and dR/dT) in the thin Au films are collected at 800 nm. The cross-correlation of the pump and probe pulses at the sample surface is measured to be ∼825 fs, as outlined in the Supporting Information. Example TDTR data on the Au/sapphire and Au/SiO_2 samples are shown in Fig. 1, along with indicators of the pump-probe delay time in which dR/dT_e and dR/dT are measured.

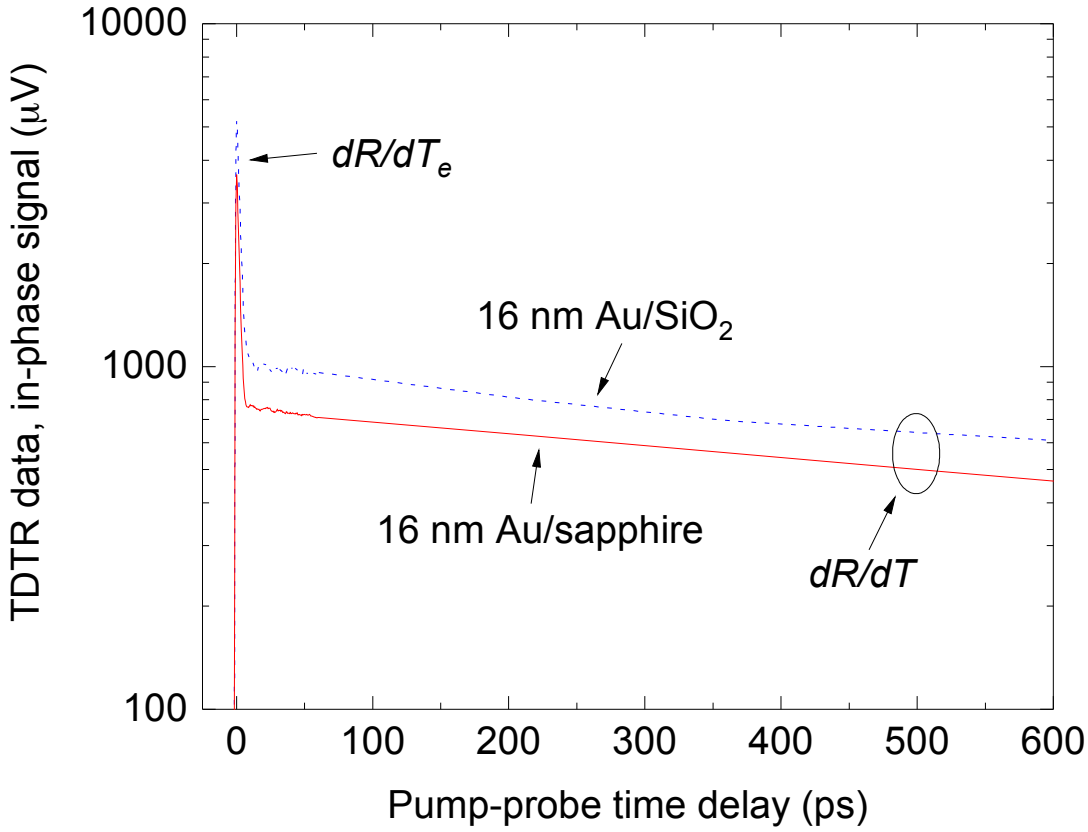

Figure 1: TDTR data for the 16 nm thin films on SiO_2 and Al_2O_3 substrates. At short timescales, the large rise in the measured change in reflectivity is associated with an electron-phonon nonequilibrium when $T_e \gg T_p$. By $\sim$ 10 ps, the electrons and phonons in gold film are thermalized and $T_e \approx T_p$ for $t > 10$ ps.

We quantify dR/dT_e (and dR/dT) using the procedure outlined in Wang *et al.*[10] In this ap-

proach, dR/dT is determined by

$$\frac{dR}{dT} = \frac{\sqrt{2}}{Q}\left[\frac{V(t)}{V_o}\right]\left[\frac{R}{\Delta T(t)}\right] \tag{7}$$

where Q is the quality factor of the LC circuit used to filter out side bands (in our system Q=10), V_o is the DC voltage measured by the photodiode, $V(t)$ is the change in voltage measured by the lock-in amplifier at some time pump-probe delay time t, R is the reflectivity of the Au film in equilibrium, and $\Delta T(t)$ is the change in temperature of the Au film induced by the absorbed pump pulse at some pump-probe delay time t. In the case of the equilibrium thermoreflectance coefficient dR/dT, which is commonly reported when $T_e \approx T_p$, $\Delta T(t)$ is determined by calculating the surface temperature predicted via the solution to the cylindrical heat equation detailed previously,[40,45] and also detailed in the Supporting Information.

As a calibration, we deposit 80 nm of Au on sapphire substrates and measure dR/dT at a pump-probe delay time of $t = 500$ ps using a range of different pump powers, the results of which are shown in Fig. 2. The value for dR/dT that we measure on the 80 nm Au/sapphire calibration for our range of fluences has a small pump power dependence, decreasing from $dR/dT = 3.74 \times 10^{-5}$ K^{-1} to $dR/dT = 3.2 \times 10^{-5}$ K^{-1}, which agrees well with previous measurements for dR/dT of gold reported by Wang *et al.*[10] and Tessier *et al.*[34] This power dependence in dR/dT is expected based on small perturbations in lattice temperature and the stipulation that $T_e \approx T_p$. We also measure this equilibrium dR/dT at $t = 500$ ps in our 16 nm Au/sapphire films at various pump powers. As seen in Fig. 2, the minor negative dependence on power at this pump-probe delay time remains, but the values for dR/dT are slightly higher than the 80 nm case (dR/dT spans $dR/dT = 4.13 \times 10^{-5}$ K^{-1} to $dR/dT = 3.57 \times 10^{-5}$ K^{-1} for these 16 nm films from 5 to 30 mW of incident pump power, respectively).

To investigate the origin of this slight difference in dR/dT of these Au/sapphire films, we characterized the structural properties of these 16 and 80 nm Au films using X-ray diffraction (XRD) and X-ray reflectivity (XRR). $\theta/2\theta$ scans measure constructive interference of x-rays in a

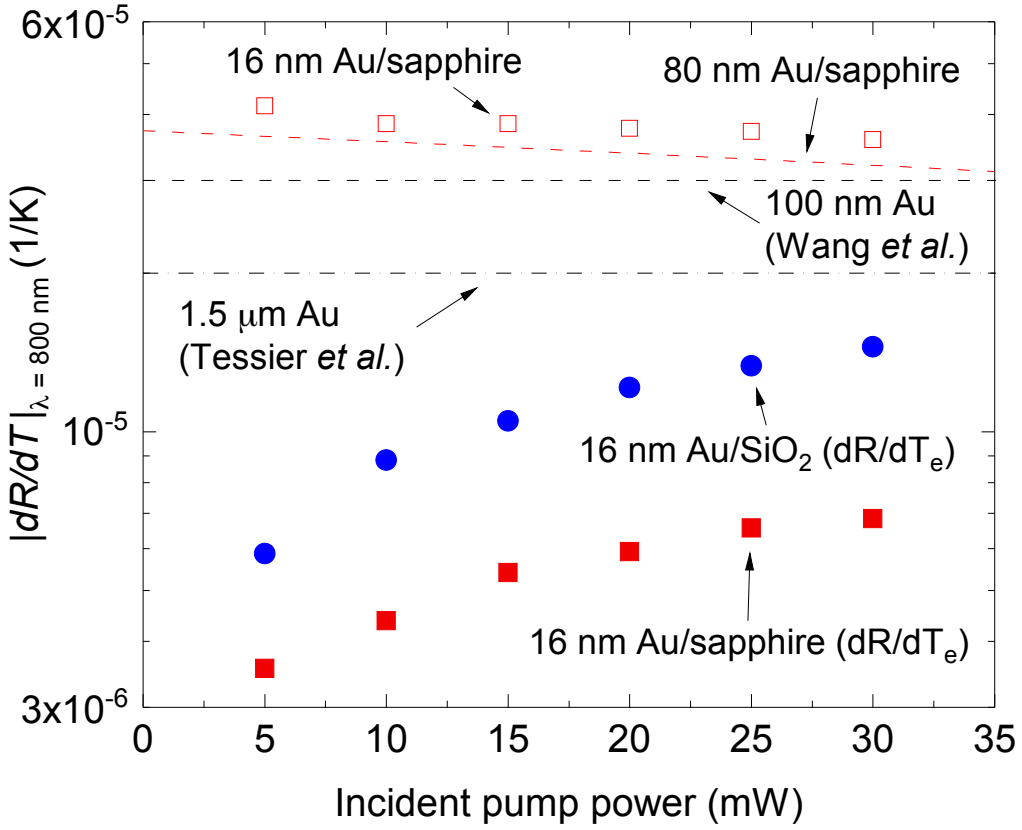

Figure 2: dR/dT_e and dR/dT measurements as a function of incident pump power for 16 nm and 80 nm of Au films on sapphire and SiO_2 substrates. dR/dT_e in the 16 nm films increase with increasing pump power density during our TDTR experiments. The value for dR/dT we measure on the 80 nm Au/sapphire calibration decreases from $dR/dT \approx 4.13 \times 10^{-5}$ K^{-1} to $dR/dT = 3.2 \times 10^{-5}$ K^{-1} at 30 mW incident pump power; these values agree well with previous measurements for dR/dT of gold reported by Wang *et al.*[10] (solid dashed line) and Tessier *et al.*[34] (solid dash-dot line). Note, we also measure a negative change in dR/dT as a function of pump power for the 16 nm Au/sapphire sample in equilibrium conditions ($T_e \approx T_p$), but a value that is slightly higher than both our 80 nm sample and the previous literature values.[10,34] This slight difference in dR/dT of these Au/sapphire calibration measurements most likely arises from the structural differences between the two films in this study, as demonstrated from our XRD and XRR analysis in Fig. 3. The thin gold film has a lower density, which may indicate a higher grain boundary density, smaller crystallite sizes, strain, or other lattice defects. These defects, in turn, may influence electron-phonon coupling to produce a finite thickness-dependent dR/dT coefficient.[55]

crystal's planes, by which we can back out information about the material's crystalline structure.

By measuring $\theta/2\theta$ scans we can determine crystallinity, grain size distribution, and strain of the

films, while ϕ-scans tell us the in-plane crystallinity. XRR is a high-angle diffraction technique with x-rays that gives us the overall film thickness.

X-ray diffraction and reflectivity patterns were collected using a PANalytical Empyrean XRD in parallel beam geometry with a Ge (220) double-bounce hybrid mirror-monochromator (1/32° divergence slit) incident optic and a 0.18° parallel plate collimator and proportional detector (Xe) as receiving optics. The XRD data in Fig. 3a and b show that the films are highly crystalline with an epitaxial (111) orientation on c-plane sapphire. Thickness fringes in the $\theta - 2\theta$ scans (Fig. 3a) indicate intense scattering at the Au/substrate interface and smooth interfaces. The RMS roughness and density of the 80 nm film are 2.3 ± 0.04 nm and 19.8 ± 0.4 g cm^{-3}, respectively, and those of the 16 nm film are 0.8 ± 0.03 nm and 19.1 ± 0.2 g cm^{-3}, respectively, as measured by XRR. Note, the thicknesses of these films are also confirmed with XRR, and for the 16 nm film, picosecond acoustics.[53,56] More information of the XRD and XRR methods employed in this work is detailed in the Supporting Information.

This slight difference in dR/dT of these Au/sapphire calibration measurements most likely arises from the structural differences between the two films in this study. The thin gold film has a lower density, which may indicate a higher grain boundary density, smaller crystallite sizes, strain, or other lattice defects. These defects, in turn, may influence electron-phonon coupling to produce a finite thickness-dependent dR/dT coefficient.[55] Our XRD results, as shown in Fig. 3a, do suggest biaxial compressive strain could be present in the thin Au films due to a slight shift in the Au (111) peak to lower 2θ, relative to the 80 nm Au film; an increase in dR/dT associated with this strain would be consistent with previous TDTR experiments on Al films where strain was determined to cause a change in the thermoreflectance coefficient.[10] A comprehensive structural analysis of Au films grown on sapphire is beyond the scope of this work, but our results imply that a material's thermoreflectance response depends, at least slightly, on its structural and defect properties, and that these properties can vary from sample to sample. Regardless of the underlying cause, there appears to be a consistent increase in dR/dT with decreasing film thickness for the values shown in Fig. 2.

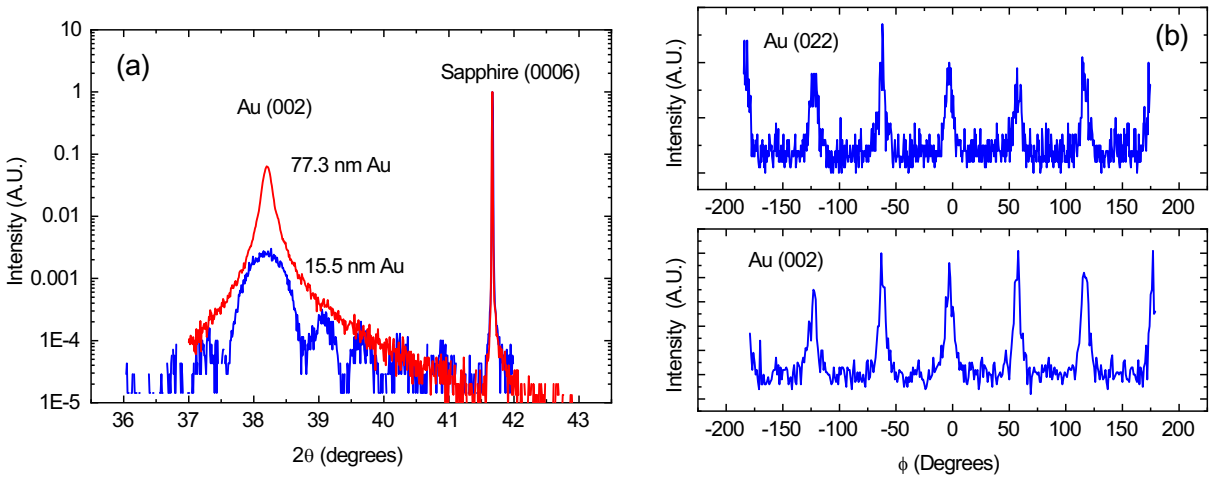

Figure 3: (a) X-ray diffraction $\theta - 2\theta$ scans of thin (blue line) and thick (red line) Au thin film samples on c-plane sapphire showing, in part, the epitaxial relationship between Au (111) planes and the basal planes of sapphire. The thickness fringes in both scans indicate smooth interfaces in the films. A slight shift of the Au (111) peak in the 15.5 nm thick sample to a lower 2θ value (38.192° vs. 38.206°) suggests that compressive biaxial strain may be present. The intensities are normalized by the sapphire (0006) reflection. (b) X-ray diffraction skew-symmetric φ scans about the Au (022) and Au (002) peaks (80 nm thick Au sample). The distinct six-fold symmetry in both scans results from in-plane crystallographic orientation and indicates epitaxial growth of (111)-oriented Au on c-plane sapphire. Note that for perfect epitaxy, three-fold symmetry would be expected. The six-fold symmetry here can be attributed to two equivalent in-plane orientations.[57]

Using Eq. 7 and replacing $\Delta T\left(t\right)$ with $\Delta T_e\left(t=0\right)$ calculated with the two temperature model (TTM),[58,59] where $t = 0$ ps is the the time delay corresponding to the peak TDTR signal and maximum electron temperature during electron-phonon nonequilibrium, we calculate dR/dT_e for the hot electrons in the Au thin film samples; details of these TTM calculations are outlined in the Supporting Information. The results of these dR/dT_e measurements are shown in Fig. 2 as a function of incident pump power. The fact that dR/dT_e depends on the incident pump power density during a TDTR experiment implies dR/dT_e exhibits a much stronger temperature dependence than dR/dT. Thus, this suggests that the hot electron reflectivity changes nonlinearly with temperature (i.e., ΔR is nonlinear with electron temperature), unlike the "equilibrium" reflectivity of a metal. This is consistent with our prior discussion in Section II and a comparison of both dR/dT_e and dR/dT in Fig 2.

Analysis of the electron temperature dependence of dR/dT_e

The theory outlined in Section II suggests that the thermoreflectance coefficient for a given material, when grown on varying substrates, could be perceived to be different if the steady state temperature rises from laser heating are not correctly accounted for. As this 'background' temperature rise associated with pulse accumulation is highly dependent on the thermal conductivity of the supporting substrate, the calculated *instantaneous* temperature rise, and thus dR/dT_e, can appear to be substrate-dependent rather than intrinsic to the thin film material, even when measured under similar laser parameters (e.g., fluence).[45] Indeed, the different values for dR/dT_e as a function of incident laser power presented in Fig. 2 allude to this fact as the nominal value increases with increasing pump power, in contrast to the trend observed under equilibrium conditions. Through the ability to measure dR/dT_e as a function of T_e during conditions of strong electron-phonon nonequilibrium (i.e., when $T_e \gg T_p$), we ensure that the electron temperature dependence of dR/dT_e should always appear linear if our theory outlined Section II is correct. Differences in dR/dT_e of the thin Au films based on the substrate could arise due to different steady state temperature rises, since the thermal conductivity of sapphire is roughly a factor of 25 greater than SiO_2. When $T_{p,\mathrm{SiO_2}} > T_{p,\mathrm{sapphire}}$, the expression in parentheses in Eq. 4 will be different for the sapphire and SiO_2 substrates. However, since $T_e \gg T_p$, this will result in dR/dT_e varying linearly with T_e but just having different slopes based on the different values for T_p resulting from the different substrate thermal conductivities.

To study this, we plot the electron temperature dependence of dR/dT_e in Fig. 4, where the electron temperature rise plotted is obtained via TTM[58,59] calculations. Clearly dR/dT_e depends on electron temperature, further demonstrating the nonlinearity of the reflectivity, ΔR, during electron-phonon nonequilibrium. Also shown are best fit trend lines to each data set, $dR/dT_e = C_1 T_e$ where C_1 is a constant, demonstrating that dR/dT_e is linear with electron temperature in each sample. While the electron temperatures in Au/SiO_2 and Au/sapphire are predicted to be relatively similar via TTM calculations, we ascribe the difference in dR/dT_e to be due to the different absolute temperatures of the samples during TDTR measurements, which arise from changes in

steady-state heating based on the different substrates.[45] This is consistent with our discussion in the beginning of this section: namely, the dR/dT_e is always linear with T_e assuming $T_e \gg T_p$, and changes in the slope of dR/dT_e vs. T_e can be due to changes in T_p.

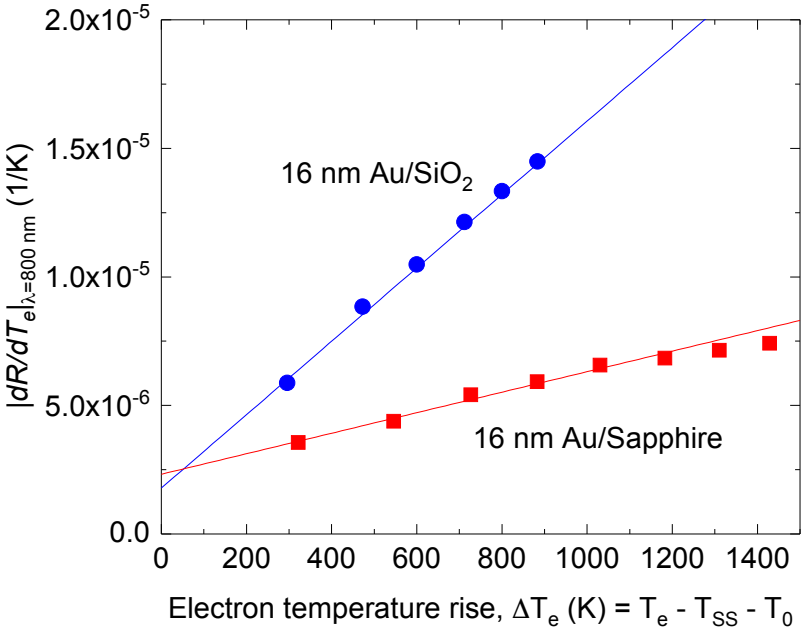

Figure 4: Hot electron thermoreflectance coefficient, dR/dT_e, of the Au/sapphire (squares) and Au/SiO_2 (circles) samples plotted as a function of electron temperature rise, ΔT_e, predicted via calculations of the TTM.[58,59] dR/dT_e of the gold films are linear with T_e assuming $T_e \gg T_p$, regardless of the substrate, and changes in the slope of dR/dT_e vs. T_e is indicative of changes in T_p.

Inelastic electron-phonon scattering rates derived from dR/dT

The thermoreflecance coefficients of metals are intimately related to the electron scattering processes through the scattering rate, $1/\tau$ in Eq. 3. As we show here, by examining the coefficients of the expansion of Eq. 3, the coefficient that describes electron-phonon scattering rates, B_{ep}, can be simply determined if dR/dT is known; we outline this approach below. However, we caution that our analysis relies on the metal exhibiting a Drude-like free electron response. Nevertheless, in principle, the extraction of electronic scattering coefficients from measurements of dR/dT is

achievable even for materials that do not obey the Drude model provided an alternative model for the optical dielectric function can be accurately determined.

Consider the thermoreflectance coefficient that describes the temperature response of the reflectivity when the electron and phonon subsystems can be defined with nearly equivalent temperatures (i.e., $T_e \approx T_p$). In this case, assuming moderate temperatures, the scattering rate term in the Drude model (Eq. 3) becomes dominated by the electron-phonon scattering rate (i.e., $A_{ee}T_e^2 \ll B_{ep}T_p$) and the Drude model becomes

$$\tilde{\epsilon}_f\left(T = T_e \approx T_p\right) = 1 - \frac{\omega_{\text{plasma}}^2}{\omega\left(\omega + iB_{ep}T\right)} \tag{8}$$

where $T = T_e \approx T_p$. Using this expression in Eq. 2, and taking the temperature derivative with respect to T and then expanding about T yields

$$\frac{dR\left(T = T_e \approx T_p\right)}{dT} \approx \sqrt{R}\left(\tilde{a} + \tilde{b}T\right) \tag{9}$$

where $\tilde{a}$ and $\tilde{b}$ are complex numbers that are functions of ω, ω_{plasma}, and B_{ep}. Thus, in a small perturbation limit where the electron-phonon subsystems are in equilibrium (e.g., the regime of which thermoreflectance spectroscopy techniques such as TDTR are used to measure thermal properties), we can use the linear change in dR/dT to determine these complex numbers. In the cases where the absolute temperature, T, is not perturbed enough to obtain this linear relationship and dR/dT was assumed to be a constant (e.g., the values reported from previous works as shown in Fig. 2), one can assume $dR/dT \approx \tilde{a}\sqrt{R}$, where

$$\tilde{a} \approx -\frac{2iB_{ep}\omega_{\text{plasma}}^2}{\omega^3\sqrt{1 - \frac{\omega_{\text{plasma}}^2}{\omega^2}}\left(1 + \sqrt{1 - \frac{\omega_{\text{plasma}}^2}{\omega^2}}\right)^2}. \tag{10}$$

Equation 10 leads to two major observations. Firstly, dR/dT in a metal can be expressed solely as a function of ω, ω_{plasma}, and B_{ep}. Secondly, with knowledge of dR/dT, the electron-phonon

scattering rates can be calculated. This offers a potentially alternative way to determine electron-phonon scattering rates in metals that does not rely on interpretation of electrical resistivity or thermal conductivity measurements. Furthermore, since dR/dT can be measured using continuous wave lasers and without inducing electron-phonon nonequilibrium, this potentially alleviates the necessity of ultrafast laser pump-probe experiments to determine electron-phonon scattering.

Using Eq. 10 with dR/dT measured on our 80 nm Au/sapphire and 16 nm Au/sapphire samples, we determine $B_{ep} = 2.34 \pm 0.26 \times 10^{11}$ s^{-1} K^{-1} and $B_{ep} = 2.94 \pm 0.22 \times 10^{11}$ s^{-1} K^{-1}, respectively. Using this same approach applied to the previous measurements of dR/dT from Wang *et al.*[10] and Tessier *et al.*[34] yields $B_{ep} = 2.03 \times 10^{11}$ s^{-1} K^{-1} and $B_{ep} = 1.35 \times 10^{11}$ s^{-1} K^{-1}, respectively. The minor differences among these various values of B_{ep} in gold are directly related to our discussion regarding the differences in the measured dR/dT discussed previously. However, we note that these dR/dT-derived values for B_{ep} are in excellent agreement with values reported for B_{ep} in Au previously that were inferred using a range of different techniques other than this thermoreflectance approach presented here ($B_{ep} = 1.23 - 3.60 \times 10^{11}$ s^{-1} K^{-1}).[47,49,52,60] Additionally, we can directly fit Eq. 8 to our measured change in reflectivity as a function of absolute temperature as a means of confirming these values; in doing so, we find $B_{ep} = 2.11 \times 10^{11}$ s^{-1} K^{-1} for the 16 nm Au film on sapphire, which is in excellent agreement with this alternative approach of using Eq. 10.

We recently reported elastic electron-phonon dephasing times in Au calculated with time-dependent density functional theory and nonadiabatic molecular dynamics.[61] We explicitly studied the role of the excited states of the electrons on this dephasing time in an effort to assess the role of electron temperature depedence on electron-phonon coupling. Based on the degree of electronic excitation, elastic dephasing times spanned from 4.3 to 7.5 fs for a room temperature lattice, which corresponds to $B_{ep} = 4.44 - 7.75 \times 10^{11}$ s^{-1} K^{-1}. Note, these rates are faster than B_{ep} in gold, as discussed above, but it's important to note our previous work predicted elastic dephasing times, where the experimental determination of B_{ep} are related to inelastic electron-phonon processes. The approach to characterize B_{ep} via analysis of the dR/dT value outlined in this work offers

a unique path forward to characterize these elastic electron-phonon interactions through control of the sample temperature or geometry to vary the relative roles of elastic and inelastic electron-phonon scattering.[62–64]

Summary

We have developed an experimental analysis to measure the "hot electron" thermoreflectance coefficient, dR/dT_e in metal films via monitoring the thermoreflectance during pump-probe measurements immediately after pulsed laser absorption. Immediately after pulse absorption during TDTR measurements of thin gold films, the electrons in the Au are out of equilibrium with the lattice, and thus the condition $T_e \approx T_p$, usually assumed while reporting dR/dT values is invalid. In this pump-probe time delay measurement regime, which is on the order of the sub-picosecond pulse duration, T_e can be much greater than T_p, allowing us to measure this hot electron thermoreflectance coefficient, dR/dT_e. Using this approach applied to thin gold films on silica glass and sapphire substrates as experimental examples, we experimentally validate the linear electron temperature dependence of the thermoreflectance coefficient. Furthermore, we demonstrate a lattice temperature dependence in dR/dT_e, suggesting the nonlinear nature of ΔR in free electron metals can also arise in part from lattice heating in addition to electron heating. Our approach outlined in this work to directly quantify dR/dT_e provides a metrology to further understand excited state scattering effects on the dielectric function of metals.

Acknowledgement

We appreciate funding from the U.S. Department of Defense, Multidisciplinary University Research Initiative through the Army Research Office, Grant No. W911NF-16-1-0406.

References

(1) Weaver, J. H.; Lynch, D. W.; Culp, C. H.; Rosei, R. Thermoreflectance of V, Nb, and paramagnetic Cr. *Physical Review B* **1976**, *14*, 459–463.

(2) Colavita, E.; Franciosi, A.; Lynch, D. W.; Paolucci, G.; Rosei, R. Thermoreflectance investigation of the antiferromagnetic and paramagnetic phases of Cr. *Physical Review B* **1983**, *27*, 1653–1663.

(3) Colavita, E.; Franciosi, A.; Mariani, C.; Rosei, R. Thermoreflectance test of W, Mo and paramagnetic Cr band structures. *Physical Review B* **1983**, *27*, 4684–4693.

(4) Lynch, D. W.; Rosei, R.; Weaver, J. H. Infrared and visible optical properties of single crystal Ni at 4 K. *Solid State Communications* **1971**, *9*.

(5) Rosei, R.; Lynch, D. W. Thermomodulation spectra of Al, Au, and Cu. *Physical Review B* **1972**, *5*, 3883–3894.

(6) Rosei, R.; Culp, C. H.; Weaver, J. H. Temperature modulation of the optical transitions involving the Fermi surface in Ag: Experimental. *Physical Review B* **1974**, *10*, 484–489.

(7) Rosei, R. Temperature modulation of the optical transitions involving the Fermi surface in Ag: Theory. *Physical Review B* **1974**, *10*, 474–483.

(8) Hostetler, J. L.; Smith, A. N.; Norris, P. M. Thin-film thermal conductivity and thickness measurements using picosecond ultrasonics. *Microscale Thermophysical Engineering* **1997**, *1*, 237–244.

(9) Hsieh, W. P.; Cahill, D. G. Ta and Au(Pd) alloy metal film transducers for time-domain thermoreflectance at high pressures. *Journal of Applied Physics* **2011**, *109*, 113520.

(10) Wang, Y.; Park, J. Y.; Koh, Y. K.; Cahill, D. G. Thermoreflectance of metal transducers for time-domain thermoreflectance. *Journal of Applied Physics* **2010**, *108*, 043507.

(11) Hopkins, P. E. Effects of electron-boundary scattering on changes in thermoreflectance in thin metal films undergoing intraband excitations. *Journal of Applied Physics* **2009**, *105*, 093517.

(12) Eesley, G. L. Observation of nonequilibrium electron heating in copper. *Physical Review Letters* **1983**, *51*, 2140–2143.

(13) Eesley, G. L. Generation of nonequlibrium electron and lattice temperatures in copper by picosecond laser pulses. *Physical Review B* **1986**, *33*, 2144–2151.

(14) Hohlfeld, J.; Wellershoff, S. S.; Gudde, J.; Conrad, U.; Jahnke, V.; Matthias, E. Electron and lattice dynamics following optical excitation of metals. *Chemical Physics* **2000**, *251*, 237–258.

(15) Hohlfeld, J.; Conrad, U.; Muller, J. G.; Wellershoff, S. S.; Matthias, E. In *Nonlinear optics in metals*; Bennemann, K. H., Ed.; Clarendon Press: Oxford, 1998; pp 219–267.

(16) Jha, S. S.; Warke, C. S. Interband contributions to optical harmonic generation at a metal surface. *Physical Review* **1967**, *153*, 751–759.

(17) Rustagi, K. C. Bilinear optical polarizability of siliver. *Il Nuovo Cimento* **1968**, *53B*, 346–362.

(18) Fann, W. S.; Storz, R.; Tom, H. W. K.; Bokor, J. Direct measurement of nonequilibrium electron-energy distributions in subpicosecond laser-heated gold films. *Physical Review Letters* **1992**, *68*, 2834–2837.

(19) Fann, W. S.; Storz, R.; Tom, H. W. K.; Bokor, J. Electron thermalization in gold. *Physical Review B* **1992**, *46*, 13592–13595.

(20) Brorson, S. D.; Kazeroonian, A.; Moodera, J. S.; Face, D. W.; Cheng, T. K.; Ippen, E. P.; Dresselhaus, M. S.; Dresselhaus, G. Femtosecond room-temperature measurement of the electron-phonon coupling constant λ in metallic superconductors. *Physical Review Letters* **1990**, *64*, 2172–2175.

(21) Groeneveld, R. H. M.; Sprik, R.; Lagendijk, A. Effect of a nonthermal electron distribution on the electron-phonon energy relaxation process in noble metals. *Physical Review B* **1992**, *45*, 5079–5082.

(22) Groeneveld, R. H. M.; Sprik, R.; Lagendijk, A. Femtosecond spectroscopy of electron-electron and electron-phonon energy relaxation in Ag and Au. *Physical Review B* **1995**, *51*, 11433–11445.

(23) Sun, C. K.; Vallee, F.; Acioli, L. H.; Ippen, E. P.; Fujimoto, J. G. Femtosecond investigation of electron thermalization in gold. *Physical Review B* **1993**, *48*, 12365–12368.

(24) Sun, C. K.; Vallee, F.; Acioli, L. H.; Ippen, E. P.; Fujimoto, J. G. Femtosecond-tunable measurement of electron thermalization in gold. *Physical Review B* **1994**, *50*, 15337–15348.

(25) Qiu, T. Q.; Tien, C. L. Size effects on nonequilibrium laser heating of metal films. *Journal of Heat Transfer* **1993**, *115*, 842–847.

(26) Qiu, T. Q.; Tien, C. L. Heat transfer mechanisms during short-pulse laser heating of metals. *Journal of Heat Transfer* **1993**, *115*, 835–841.

(27) Hopkins, P. E.; Klopf, J. M.; Norris, P. M. Influence of interband transitions on electron-phonon coupling measurements in Ni films. *Applied Optics* **2007**, *46*, 2076–2083.

(28) Hopkins, P. E.; Kassebaum, J. L.; Norris, P. M. Effects of electron scattering at metal-nonmetal interfaces on electron-phonon equilibration in gold films. *Journal of Applied Physics* **2009**, *105*, 023710.

(29) Hopkins, P. E.; Norris, P. M. Substrate influence in electron-phonon coupling measurements in thin Au films. *Applied Surface Science* **2007**, *253*, 6289–6294.

(30) Hopkins, P. E.; Duda, J. C.; Petz, C. W.; Floro, J. A. Controlling thermal conductance through quantum dot roughening at interfaces. *Physical Review B* **2011**, *84*, 035438.

(31) Hopkins, P. E.; Phinney, L. M.; Serrano, J. R. Reexamining electron-Fermi relaxation in gold films with a nonlinear thermoreflectance model. *Journal of Heat Transfer* **2011**, *133*, 044505.

(32) Hostetler, J. L.; Smith, A. N.; Czajkowsky, D. M.; Norris, P. M. Measurement of the electron-phonon coupling factor dependence on film thickness and grain size in Au, Cr, and Al. *Applied Optics* **1999**, *38*, 3614–3620.

(33) Caffrey, A. P.; Hopkins, P. E.; Klopf, J. M.; Norris, P. M. Thin film non-noble transition metal thermophysical properties. *Microscale Thermophysical Engineering* **2005**, *9*, 365–377.

(34) Tessier, G.; Holé, S.; Fournier, D. Quantitative thermal imaging by synchronous thermoreflectance with optimized illumination wavelengths. *Applied Physics Letters* **2001**, *78*, 2267–2269.

(35) Humbert, A.; Debever, J. M.; Hanus, J.; Dourdan, C. Low energy interband transitions in aluminium. *Journal de Physique Lettres* **1977**, *38*, 479–481.

(36) Hanus, J.; Feinleib, J.; Scouler, W. J. Low-energy interband transitions and band structure in nickel. *Physical Review Letters* **1967**, *19*, 16–20.

(37) Hopkins, P. E.; Serrano, J. R.; Phinney, L. M.; Kearney, S. P.; Grasser, T. W.; Harris, C. T. Criteria for cross-plane dominated thermal transport in multilayer thin film systems during modulated laser heating. *Journal of Heat Transfer* **2010**, *132*, 081302.

(38) Cheaito, R.; Gorham, C. S.; Misra, A.; Hattar, K.; Hopkins, P. E. Thermal conductivity measurements via time-domain thermoreflectance for the characterization of radiation induced damage. *Journal of Materials Research* **2015**, *30*, 1403–1412.

(39) Hopkins, P. E. Thermal transport across solid interfaces with nanoscale imperfections: Effects of roughness, disorder, dislocations, and bonding on thermal boundary conductance. *ISRN Mechanical Engineering* **2013**, *2013*, 682586.

(40) Cahill, D. G. Analysis of heat flow in layered structures for time-domain thermoreflectance. *Review of Scientific Instruments* **2004**, *75*, 5119–5122.

(41) Schmidt, A. J. Pump-probe thermoreflectance. *Annual Review of Heat Transfer* **2013**, *16*, 159–181.

(42) Wilson, R. B.; Apgar, B. A.; Martin, L. W.; Cahill, D. G. Thermoreflectance of metal transducers for optical pump-probe studies of thermal properties. *Optics Express* **2012**, *20*, 28829–28838.

(43) Rost, C. M.; Ferri, K.; Braun, J. L.; Backman, L.; Opila, E.; Maria, J.-P.; Hopkins, P. E. Hafnium nitride films for thermoreflectance transducers at high temperatures: Thermal properties and potential for laser-based temperature control. *Applied Physics Letters* **2017**, *111*, 151902.

(44) Heilpern, T.; Manjare, M.; Govorov, A. O.; Wiederrecht, G. P.; Gray, S. K.; Harutyunyan, H. Determination of hot carrier energy distributions from inversion of ultrafast pump-probe reflectivity measurements. *Nature Communications* **2018**, *9*.

(45) Braun, J. L.; Hopkins, P. E. Upper limit to the thermal penetration depth during modulated heating of multilayer thin films with pulsed and continuous wave lasers: A numerical study. *Journal of Applied Physics* **2017**, *121*, 175107.

(46) Schmidt, A. J.; Chen, X.; Chen, G. Pulse accumulation, radial heat conduction, and anisotropic thermal conductivity in pump-probe transient thermoreflectance. *Review of Scientific Instruments* **2008**, *79*, 114902.

(47) Hopkins, P. E.; Duda, J. C.; Kaehr, B.; Wang Zhou, X.; Peter Yang, C.-Y.; Jones, R. E. Ultrafast and steady-state laser heating effects on electron relaxation and phonon coupling mechanisms in thin gold films. *Applied Physics Letters* **2013**, *103*, 211910.

(48) Hopkins, P. E. Influence of electron-boundary scattering on thermoreflectance calculations after intra- and interband transitions induced by short-pulsed laser absorption. *Physical Review B* **2010**, *81*, 035413.

(49) Smith, A. N.; Norris, P. M. Influence of intraband transitions on the electron thermoreflectance response of metals. *Applied Physics Letters* **2001**, *78*, 1240–1242.

(50) Hopkins, P. E. Thermoreflectance dependence on Fermi surface electron number density perturbations. *Applied Physics Letters* **2010**, *96*, 041901.

(51) Kaveh, M.; Wiser, N. Electron-electron scattering in conducting materials. *Advances in Physics* **1984**, *33*, 257–372.

(52) Guo, L.; Hodson, S. L.; Fisher, T. S.; Xu, X. Heat Transfer Across Metal-Dielectric Interfaces During Ultrafast-Laser Heating. *Journal of Heat Transfer* **2012**, *134*, 042402.

(53) Thomsen, C.; Strait, J.; Vardeny, Z.; Maris, H. J.; Tauc, J.; Hauser, J. J. Coherent phonon generation and detection by picosecond light pulses. *Physical Review Letters* **1984**, *53*, 989–992.

(54) Ghotbi, M.; Ebrahim-Zadeh, M.; Majchrowski, A.; Michalski, E.; Kityk, I. V. High-average-power femtosecond pulse generation in the blue using BiB_3O_6. *Optics Letters* **2004**, *29*, 2530–2532.

(55) Giri, A.; Gaskins, J. T.; Donovan, B. F.; Szwejkowski, C.; Warzoha, R. J.; Rodriguez, M. A.; Ihlefeld, J.; Hopkins, P. E. Mechanisms of nonequilibrium electron-phonon coupling and thermal conductance at interfaces. *Journal of Applied Physics* **2015**, *117*, 105105.

(56) Thomsen, C.; Grahn, H. T.; Maris, H. J.; Tauc, J. Surface generation and detection of phonons by picosecond light pulses. *Physical Review B* **1986**, *34*, 4129–4138.

(57) Kastle, G.; Boyen, H.-G.; Koslowski, B.; Plettl, A.; Weigl, F.; Ziemann, P. Growth of thin,

flat, epitaxial (111) oriented gold films on c-cut sapphire. *Surface Science* **2002**, *498*, 168–174.

(58) Anisimov, S. I.; Kapeliovich, B. L.; Perel'man, T. L. Electron emission from metal surfaces exposed to ultrashort laser pulses. *Journal of Experimental and Theoretical Physics (Zhurnal Eksperimentalnoi i Teoreticheskoi Fiziki)* **1974**, *39*, 375–377.

(59) Giri, A.; Gaskins, J. T.; Foley, B. M.; Cheaito, R.; Hopkins, P. E. Experimental evidence of excited electron number density and temperature effects on electron-phonon coupling in gold films. *Journal of Applied Physics* **2015**, *117*, 044305.

(60) Wang, X. Y.; Riffe, D. M.; Lee, Y.-S.; Downer, M. C. Time-resolved electron-temperature measurement in a highly excited gold target using femtosecond thermionic emission. *Physical Review B* **1994**, *50*, 8016–1019.

(61) Zhou, X.; Li, L.; Dong, H.; Giri, A.; Hopkins, P. E.; Prezhdo, O. V. Temperature Dependence of Electron-Phonon Interactions in Gold Films Rationalized by Time-Domain Ab Initio Analysis. *The Journal of Physical Chemistry C* **2017**, *121*, 17488–17497.

(62) Ptitsina, N. G.; Chulkova, G. M.; Il'in, K. S.; Sergeev, A. V.; Pochinkov, F. S.; Gershenzon, E. M.; Gershenson, M. E. Electron-phonon interaction in disordered metal films: The resistivity and electron dephasing rate. *Physical Review B* **1997**, *56*, 10089–10096.

(63) Sergeev, A. V. Electronic Kapitza conductance due to inelastic electron-boundary scattering. *Physical Review B* **1998**, *58*, R10199.

(64) Sergeev, A.; Mitin, V. Electron-phonon interaction in disordered conductors: Static and vibrating scattering potentials. *Physical Review B* **2000**, *61*, 6041–6047.

Graphical TOC Entry

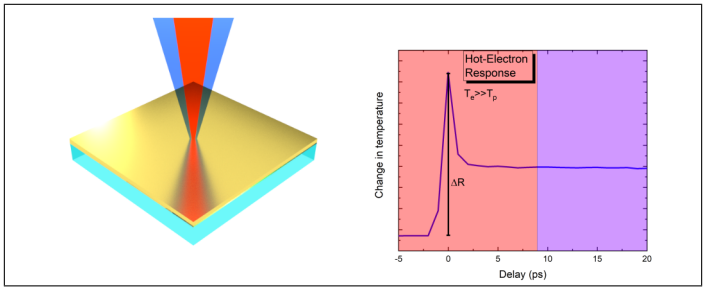

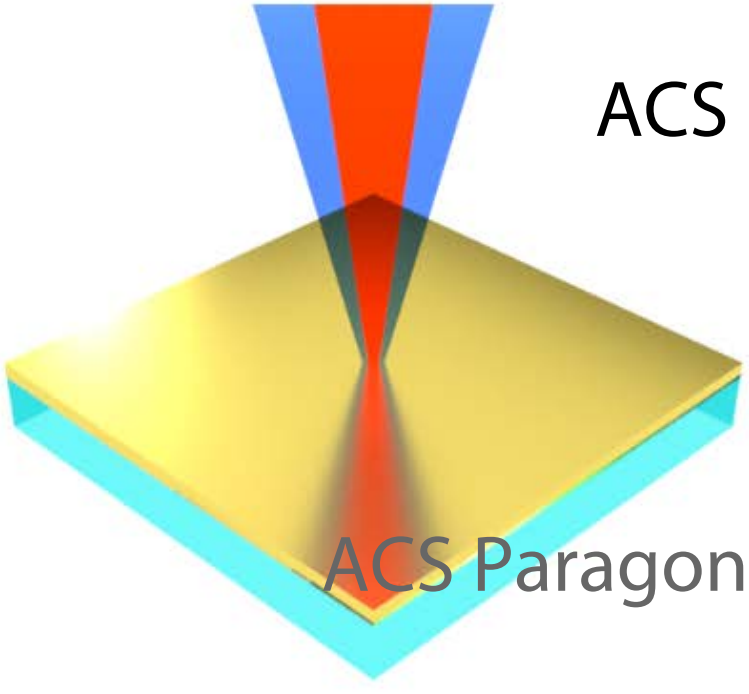

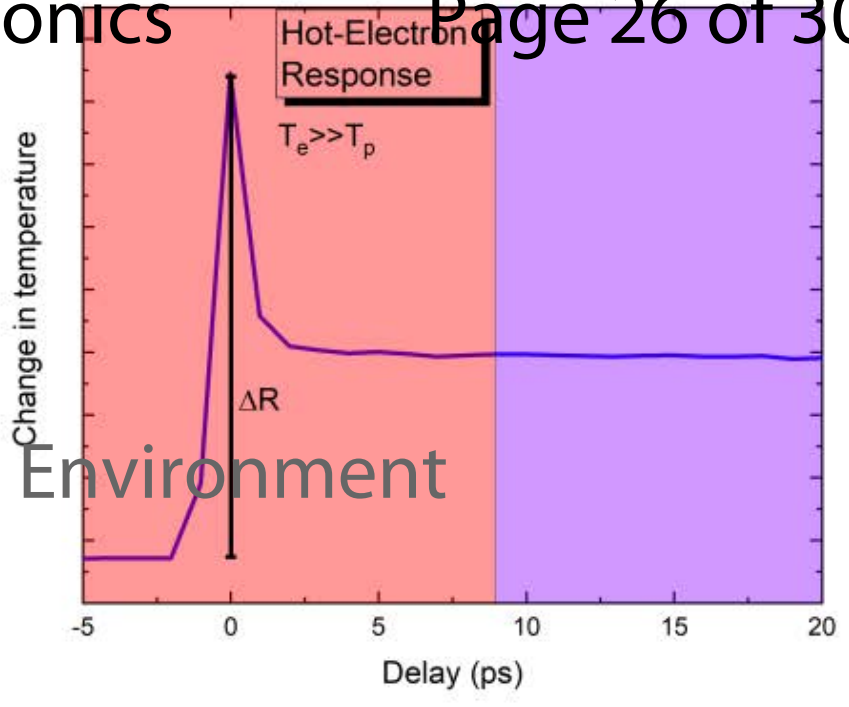

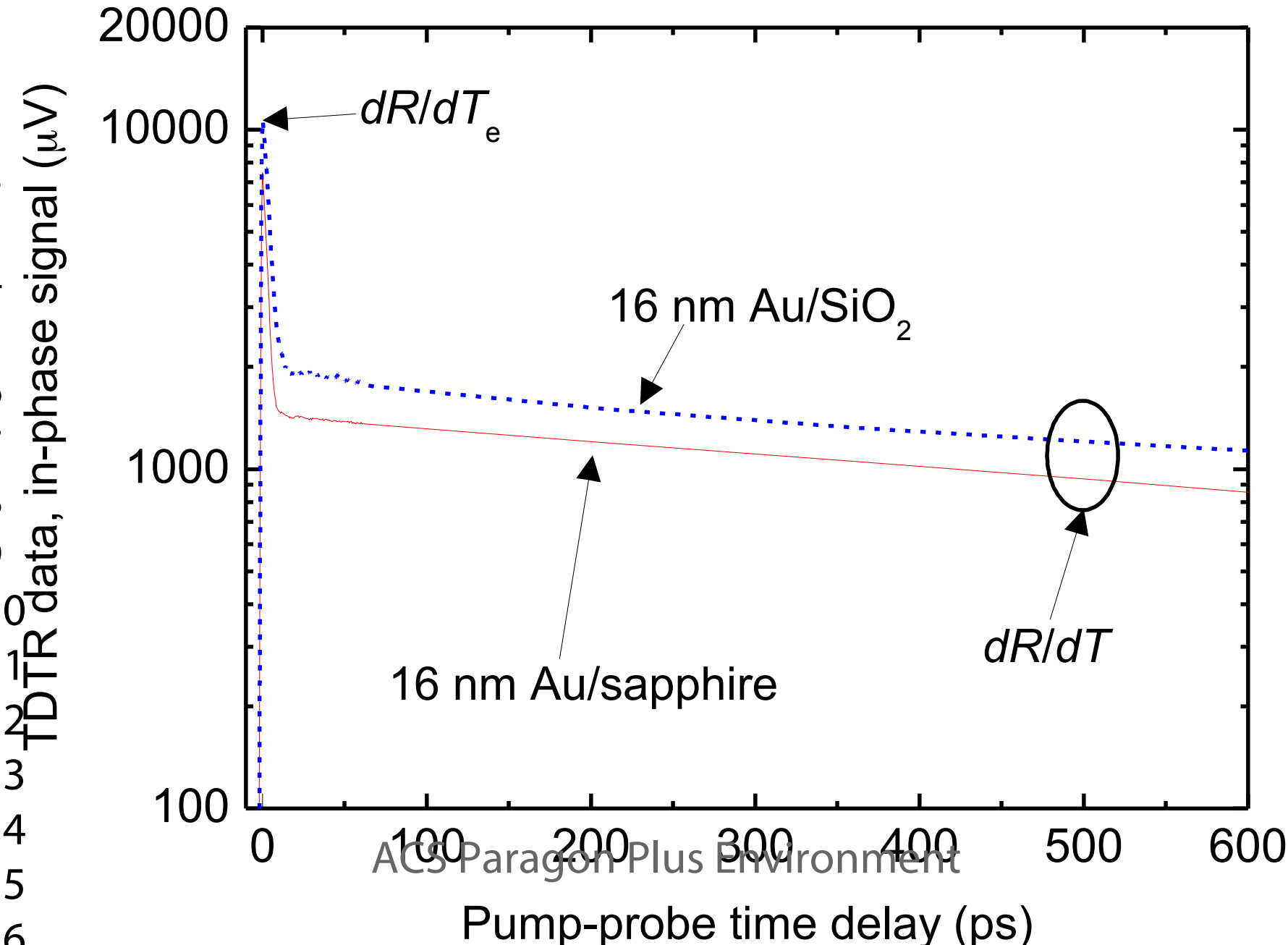

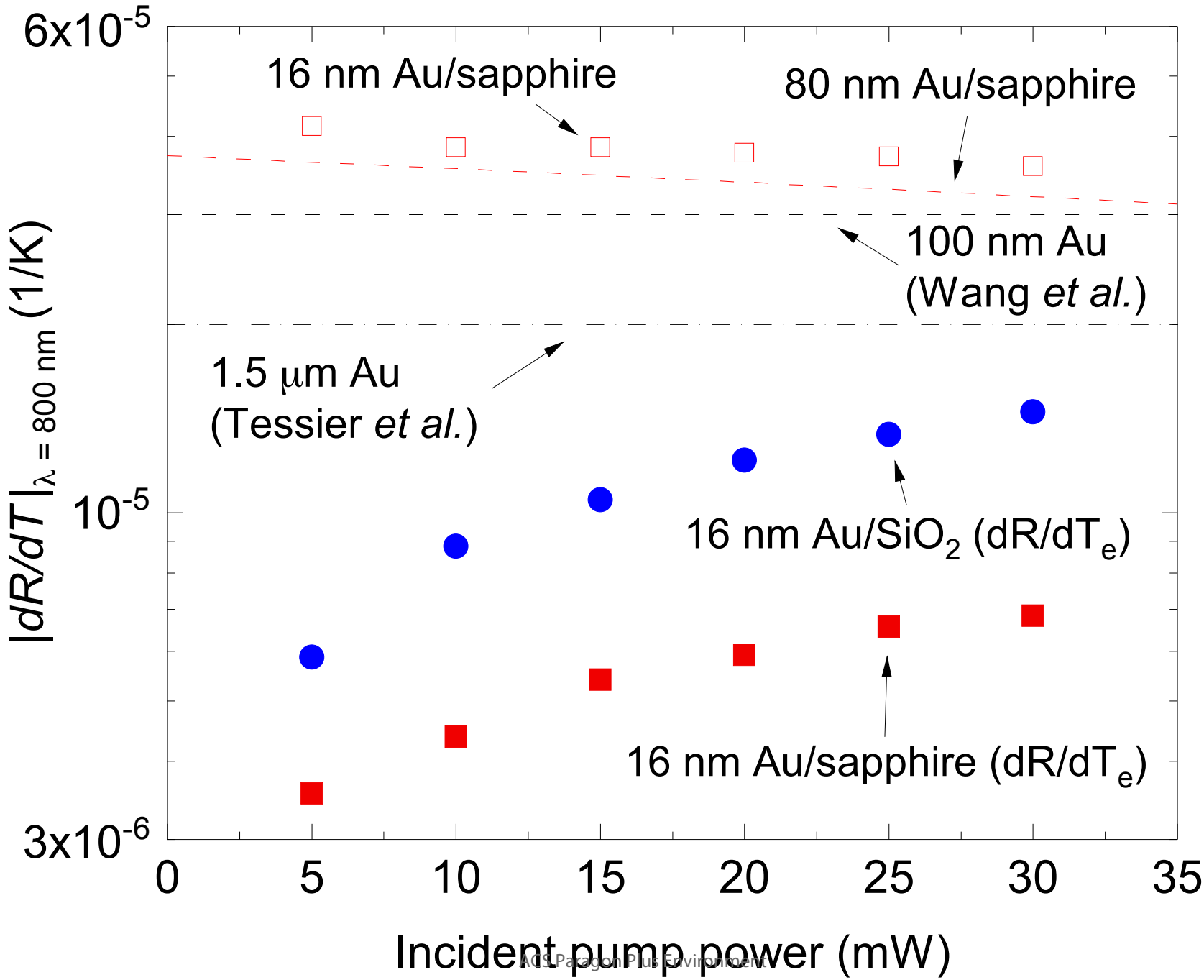

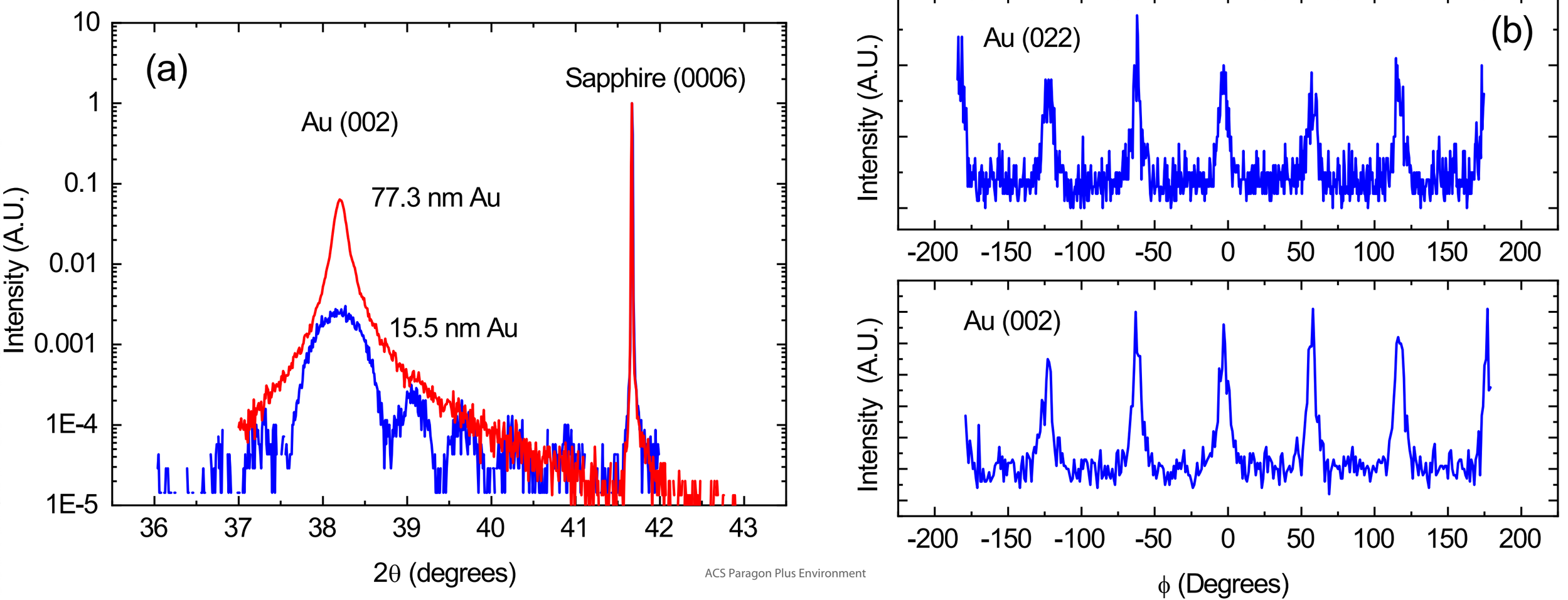
(a)
Sapphire (0006)
Au (002)
77.3 nm Au
15.5 nm Au
Intensity (A.U.)
10
1
0.1
0.01
0.001
1E-4
1E-5
36
37
38
39
40
41
42
43
2θ (degrees)
(b)
Au (022)
Intensity (A.U.)
-200
-150
-100
-50
0
50
100
150
200
Au (002)
Intensity (A.U.)
ϕ (Degrees)